Lean blowoff dynamics in bluff body stabilized flames: unsupervised classification and balance analysis

Thomas Lesaffre[a,*], Jonathan Wirtz[a], Eleonore Riber[a], Bénédicte Cuenot[a], Quentin Douasbin[a]

[a] *CERFACS, 42 Avenue Gaspard Coriolis, Toulouse Cedex 1, 31057, France*

Abstract

Lean blow-out (LBO) is a critical phenomenon in gas turbines. It is enhanced by very to ultra-lean operating conditions which are considered today to decrease the environmental impact of combustion. Despite many studies on the subject, the physical mechanisms leading to global flame extinction are not fully understood. Recently, unsupervised classification has appeared in the literature as an efficient tool to identify key features in reactive flows. In this work, unsupervised classification relying on Principle Component Analysis (PCA) and K-means clustering algorithms is used to investigate the underlying mechanisms of a blowoff event in a bluff body configuration. The unsupervised classification allows to identify and track in time 4 distinct zones: fresh gases, burnt gases, fast reacting flame and preheat zone. To elucidate the blow-out processes, an analysis of mass and energy balances of the different zones is proposed. This analysis describes the temporal evolution of the zones as a result of their interactions, which is the main driver for flame stabilization or blowoff. For the considered blowoff event, the extinction is induced by an imbalance between the various contributions identified by the proposed analysis: while the decrease in fuel mass flow rate modifies both the conductive fluxes and chemistry source terms in the reactive zones, the convective fluxes remain constant over time as the total mass flow rate is kept constant. This work suggests that the proposed methodology is a useful tool to analyze unsteady configurations and understand the main mechanisms at work in such configurations.

Keywords: Lean blow-out; Principal component analysis; K-means; Numerical Combustion

1) Novelty and Significance Statement

The novelty of this research relies in the use of unsupervised classification to study the lean blow-out phenomenon. Unsupervised classification has already been used to study MILD combustion (e.g. Li et al., *Proc. Combust. Inst.* 38, 2021). In this work, the unsupervised classification methodology is extended with a balance analysis to extract physical information on the flow dynamics. This is a significant contribution because it proposes an efficient tool to analyze lean blow-out in complex flows, which remains a challenge and has no equivalent in the literature. Furthermore, the proposed methodology could be extended to study many other combustion processes.

2) Author Contributions

- TL : Conceptualization, Methodology, Formal analysis, Writing - Original Draft
- JW : Conceptualization, Methodology, Writing - Review Editing
- ER : Conceptualization, Writing - Review Editing, Supervision
- BC : Conceptualization, Writing - Review Editing, Supervision
- QD : Conceptualization, Methodology, Formal analysis, Writing - Review Editing, Supervision

1. Introduction

Modern gas turbines aim for lower NOx emissions by operating in very lean conditions, at the price of a higher risk to reach the Lean blow-out (LBO) limit [1] and quench. This raises safety concerns in aeronautical engines and demands costly procedures for land-based power generation turbines. Consequently, important efforts have been made by the community to a better understanding on the blowoff phenomenon [2, 3].

First contributions to the blowoff phenomenon focused on bluff body flames. Early studies primarily relied on experiments to propose semi-empirical correlations from experimental data and Perfectly Stirred Reactor (PSR) assumptions [4]. In the pioneer works on the blowoff phenomenom, two main methodologies to study LBO were derived, either based on PSR [5] or Characteristic Time (CT) [6]. In PSR models, the recirculation zone behind the bluff body is interpreted as a PSR: the fresh mixture coming from the shear layer mixes instantaneously with the mixture already in the recirculation zone. In this framework, LBO occurs when the energy released in the recirculation zone is not sufficient to heat the fresh mixture up to its ignition temperature. On the other hand, CT models consider that LBO occurs if the contact time in the shear layer between the hot recirculating mixture and the fresh mixture is not long enough to heat up the latter to the ignition temperature. More recently, Wang et al. [7] combined PSR and CT approaches to study the LBO of a gas turbine combustor. In their methodology the reaction zone is identified and described as a collection of PSRs.

As pointed out by Shanbhogue et al [2], all these methods can be expressed in terms of a Damköhler number $\mathrm{Da} = \tau_{\mathrm{flow}}/\tau_{\mathrm{chem}}$, as they describe the local competition between fluid mechanics and chemical processes, and are particularly well suited to identify local extinctions. However they do not consider the overall energy balance of the flame and therefore cannot predict directly global blowoff.

To study global extinction, Sturgess et al. [8] proposed to describe a combustor with a reactor network, which is a simplification often made in the literature [9, 10]. However, the identification of the different zones corresponding to the individual reactors remains a tedious work, especially when considering their volume and location fixed in time while the combustor dynamics are unsteady for stabilized flames and fully transient during an extinction event. To overcome the limitation of predefined zones, the use of unsupervised machine learning clustering algorithms have been recently proposed in the literature [11, 12].

Unsupervised classification algorithms consist in reducing the dimensionality of the variables and clustering the data [11]. Such methods have already been used to derive combustion model, for example by Savarese et al. [12] to automatically generate chemical reactor networks or by Malik et al. [13] to generate the manifold variables of the Direct Numerical Simulation of a turbulent premixed NH3/air flame. These methods also proved to be very useful to identify key features in reactive flows [11]. They were used by Zhang et al. [14], coupled with a neural network, to identify combustion regimes in turbulent non-premixed flames. Doan et al. [15] and Li et al. [16] studied MILD combustion with the help of unsupervised clustering and advanced analysis methods.

In this paper it is proposed to use classification algorithms to study LBO. The methodology is applied to a bluff body configuration, the VOLVO experiment [17], to demonstrate its capability to explain the driving mechanisms leading to flame blowoff. The methodology is in two steps: first, unsupervised clustering is used to identify the key features of the reacting flow; then, a balance analysis on the classification is performed to help understanding the blowoff process.

The remainder of this paper is organized as follows. The details of the methodology are provided in Section 2. The test case, numerical set-up and models are described in Section 3. The results are discussed in Section 4.

2. Methodology

2.1. Unsupervised classification

Unsupervised classification is proposed here to pinpoint coherent flow zones to study complex flows with a large amount of variables in both space and time (high data dimensionality). Dimensionality reduction is first applied. Then clustering divides the control volume into subdomains, providing a way to identify and study the coherent flow zones.

Dimensionality reduction is used to sort data and identify a limited set of variables that can accurately describe the problem. To this purpose, the Principal Component Analysis (PCA) is widely used in the literature [13–15], where the Principal Components (PCs) are built from a linear combination of the original data to form an orthogonal basis. PCA is briefly recalled below.

Consider a data set X of dimension $(n \times p)$ containing n samples of p variables, centered and scaled as :

$$X^c_{n,p} = \frac{X_{n,p} - \overline{X_p}}{\sigma_p} \tag{1}$$

with $\overline{X_p}$ and σ_p the mean and standard deviation of X, PCA provides q linear combinations corresponding to the eigenvectors of a covariance matrix computed from the original data matrix X_c, such that

$$X_q = Z_q A_q^t \tag{2}$$

with X_q ($n\times$p) the approximation of X^c based on the first q eigenvectors, Z_q $(n \times q)$ the principal component scores, A_q $(p \times q)$ the matrix of the first q eigenvectors and the notation ^{t} for the transposed.

The clustering is applied in cascade with the PCA in the PC plane. The number of eigenvectors q used for the clustering of the data corresponds to a cumulative explained variance of at least 95%. This is 1) necessary to identify and retain only significant variables to reduce biases in the methodology, 2) useful to optimize the performance of the chosen clustering algorithm as its time complexity is $O(n \times q \times i)$, i being the number of iterations for the clustering convergence [18].

Clustering algorithms are widely spread in the literature to classify data [12–15]. They are able to group unlabeled data that show some form of similarity. In this work, the K-means algorithm is chosen. K-means is a partition-type algorithm that classifies the data into a prescribed number of clusters, K. Starting with K randomly defined centroids, the data are associated to the cluster with the nearest centroid. Then, the position of the centroids is iteratively updated to minimize the mean of the Euclidean distance between the data in a cluster and its centroid. The objective function f to be minimized is expressed as:

$$f = \sum_{i=1}^{K} \sum_{j=1}^{m} d_{ij} \ , \text{ with } d_{ij} = ||x_j^i - c_i||^2 \quad (3)$$

where d_{ij} is the Euclidean distance between the j-th point in the i-th cluster and the centroid of the i-th cluster.

The number of clusters in the K-means algorithm is prescribed by the user. Statistical metrics have been developed in the literature to help choose the most representative number of clusters as, for instance, the silhouette plot [19]. These metrics typically characterize the data dispersion within clusters, the distance between clusters or both.

2.2. Balances

To investigate the dynamics of the main flow features, a balance analysis is performed on the clusters. The rate of change of a conserved quantity q is defined in the differential form as:

$$\frac{\partial q}{\partial t} = -\nabla \cdot (qu) - \nabla \cdot (J) + \dot{S} \quad (4)$$

where u is the velocity, $\nabla \cdot (J)$ is the diffusion term and $\dot{S}$ is a volume source term.

The above equation can be integrated over a cluster volume V_i and transformed with the divergence theorem as:

$$\int_{V_i} \frac{\partial q}{\partial t} dv = -\int_{S_i} (qu + J) \cdot n ds + \int_{V_i} \dot{S} dv \quad (5)$$

with S_i the surface area of cluster i.

The rate of change in the cluster i (LHS of Eq. 5) can then be explained by the contribution of the different terms in the RHS of Eq. 5. As the cluster volume V_i varies in time, the contributions are studied by unit volume to avoid biases due to cluster volume variation. The balance analysis studies particularly the contributions of the different terms and how they vary with time as the mean value of the quantities remains, by definition, close to the centroid of the encompassing cluster.

In this work, the rate of change of the total energy and species mass fractions are particularly investigated. The rate of change of the mass fraction Y_k of species k is:

$$\frac{\partial \rho Y_k}{\partial t} = -\nabla \cdot (\rho u Y_k) - \nabla \cdot (\rho V_{j,k} Y_k) + \dot{\omega}_k \quad (6)$$

with $-\nabla \cdot (\rho u Y_k)$ the convective flux, $-\nabla \cdot (\rho V_{j,k} Y_k)$ the diffusive flux, and $\dot{\omega}_k$ the chemical source term of species k.

In the absence of body forces, the rate of change of the total energy is:

$$\begin{aligned} \frac{\partial \rho E}{\partial t} = &-\nabla \cdot (\rho u E) - \nabla \cdot (-\lambda \frac{\partial T}{\partial x_i}) \\ &- \nabla \cdot (\rho V_{j,k} h_k) + \dot{\omega}_T \\ &+ \nabla \cdot (\sigma_{ij} u_i) \end{aligned} \quad (7)$$

with $-\nabla \cdot (\rho u E)$ the convective flux, $-\nabla \cdot \left(-\lambda \frac{\partial T}{\partial x_i}\right)$ the conductive heat flux, $-\nabla \cdot (\rho V_{j,k} h_k)$ the diffusive flux due to the diffusion of species with different enthalpies, $\dot{\omega}_T$ the energy source term, and $\nabla \cdot (\sigma_{ij} u_i)$ the flux coming from the viscous term. As the energy flux due to the viscous term is found negligible, it will not be included in the analysis, as usually done in the literature [20]. This also holds for the diffusive flux associated to the species diffusion, which will be therefore omitted in the analysis.

The objective of the balance analysis is to identify which terms in Eqs. 6 and 7 are involved in the flame stabilization and which are responsible for the LBO.

3. VOLVO test case

The studied configuration is the VOLVO combustor [17], widely used to evaluate turbulent combustion models [21]. It is a straight channel with a rectangular cross-section (0.12 m x 0.24 m). The length of the channel is 1.55 m. The bluff body has an equilateral triangular section of 0.04 m in height.

The simulation was performed with the code AVBP developed at Cerfacs [22], which solves the 3D compressible reactive Navier-Stokes equations using the Large Eddy Simulation (LES) approach. A central-finite volume Lax-Wendroff scheme [23] of 2nd order both in time and space is used to discretize convective terms, and a single Runge-Kutta step is used to explicitely integrate over time. A 2nd order finite element scheme is used for diffusive terms. LES equations are closed by the WALE subgrid-scale model [24]. Subgrid flame-turbulence interactions are taken into account by the TFLES model with a relaxation sensor [25] coupled with the Charlette constant

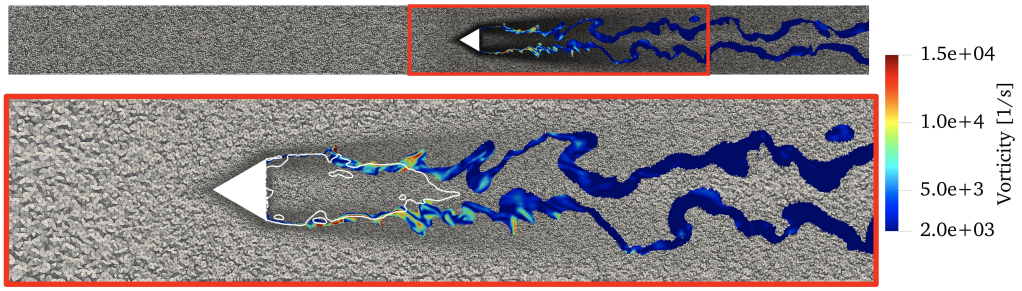

Fig. 1: Computational domain (top) and window of interest for the analysis (bottom) highlighted with a red frame. The vorticity field is shown for reactive zones (HRR > 0.1 MJ/kg/m^3). White isoline : $u = 0$ m/s.

efficiency model [26]. The NSCBC approach [27] is used for the inlet and outlet boundary conditions and a no-slip adiabatic condition is set at the walls. The chemistry, particularly suited to predict laminar flame velocity and final temperature and products in the lean combustion regime that is encountered here, is described by a 2-step scheme [28]. The above numerical method was assessed in this configuration by Rochette et al. [29]. They show a reasonable agreement, though not as precise as higher-order schemes and detailed chemistry. However, they recover most physical features of the flow, which is enough as our goal is to demonstrate the analysis methodology's potential rather than quantitatively characterizing the VOLVO rig's blowoff limit.

The mesh contains 11.9 million nodes and 68.7 million tetrahedral elements. The data that will be analyzed by unsupervised clustering corresponds to a window of 0.5 m length around the bluff body, which contains the entire recirculation zone. The mesh and the window of interest are displayed in Fig. 1.

The procedure to simulate LBO is as follows. A perfectly premixed mixture of propane-air is injected at an equivalence ratio of $\phi = 0.65$ to first stabilize the flame. Then, a step of equivalence ratio is imposed at the inlet to go from $\phi = 0.65$ to $\phi = 0.50$. This corresponds to a reduction of the laminar flame speed by a factor 2 [29]. When the variation of equivalence ratio reaches the leading edge of the bluff body, solutions are saved at a sampling of 0.7 ms until the flame blows off. The simulation is performed for a physical time of 28 ms until the flame has fully disappeared, so that 40 unsteady 3D solutions are used as a database for the analysis. Therefore, the entire space-time data is used for the PCA and, thus, the clustering.

4. Results

4.1. Application of unsupervised clustering

Two sets of variables are used and compared. The first set only provides thermo-chemical variables, case A: T and Y_k of the 5 reactive species of the scheme; N2 is not provided as it is inert and its mass fraction can be computed as a linear combination of the others. The second set, case B, considers all the variables of the reactive flow equations, i.e., 10 variables (ρ, u, v, w, Y_k and T in their non-conservative form). The obtained cumulative explained variance is displayed in Fig. 2 for both cases. For case A, 2 PCs explain 99.5% of the variance whereas 5 PCS are required to explain more than 95% of the variance for case B.

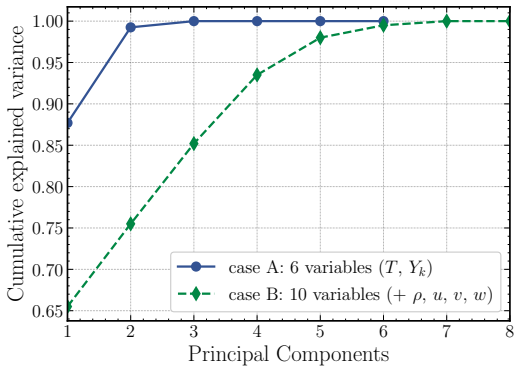

Fig. 2: Cumulative explained variance by the Principal Components for cases A and B.

The eigenvectors of the PCs are presented in Table 1 and Table 2 for case A and B respectively. For case A, the first PC represents a progress variable from the thermo-chemical point of view: the variables that decrease in the flame front have a negative coefficient value (Y_{C3H8}, Y_{O2}) whereas the ones that see an increase in their value have a positive coefficient (Y_{CO2}, Y_{H2O} and T). The behavior of PC1 for case B is the same, with the particular feature that the axial velocity is also correlated to PC1. This can be linked to the variation in axial velocity as its main change is a decrease in the recirculation zone and in the wake behind the bluff body. Both locations contain burnt gases. Hence, the axial velocity has a global evolution similar to a reactant. Second and third PCs for case B are correlated to the transverse velocity components. They represent the perturbation induced by the bluff body and the turbulence as the flow is initially injected only in the axial direction. Those PCs are not captured for case A as only thermo-chemical variables were considered. Finally, the fourth and fifth PCs for case B are mainly correlated to the axial velocity and CO mass fraction: these 2 PCs may be correlated to the intense flame zone where CO is mainly produced and located in the shear layer where axial velocity variations exist. A high correlation with

CO is also found for the second PC of case A: CO is the only thermo-chemical variable that has a behavior slightly different from a progress variable as CO mass fraction peaks in the reaction zone.

Table 1: Eigenvectors obtained from the PCA for case A.

Variable	PC1	PC2
Y_{C3H8}	-0.42	0.17
Y_{CO}	0.26	0.96
Y_{CO2}	0.43	-0.12
Y_{H2O}	0.43	-0.1
Y_{O2}	-0.43	0.1
T	0.43	-0.1

Table 2: Eigenvectors obtained from the PCA for case B.

Variable	PC1	PC2	PC3	PC4	PC5
Y_{C3H8}	-0.38	0	0	0.06	0.14
Y_{CO}	0.22	-0.01	-0.01	0.84	0.5
Y_{CO2}	0.39	0	0	-0.01	-0.14
Y_{H2O}	0.39	0	0	0	-0.13
Y_{O2}	-0.39	0	0	0	0.14
T	0.39	0	0	0	-0.14
ρ	-0.36	0.01	0	0.03	0.16
u	-0.27	-0.01	-0.01	0.54	-0.8
v	0.01	0.65	0.76	0.02	-0.01
w	0	0.76	-0.65	0	0

The silhouette scores plotted in Fig. 3 are used to find the number of clusters for the analysis. The maximum score is obtained for 2 clusters: the distinction between fresh and burnt gases is clear in both cases. However, high silhouette scores are still obtained for higher numbers of clusters. For case A, 3 and 4 clusters have a silhouette score close to 2 clusters and may be considered. For case B, 3 clusters provide a score close to the maximum. Note also the peak for 5 clusters. To further understand what the clusters represent, they are shown in Fig. 4 for both cases and different numbers of clusters K.

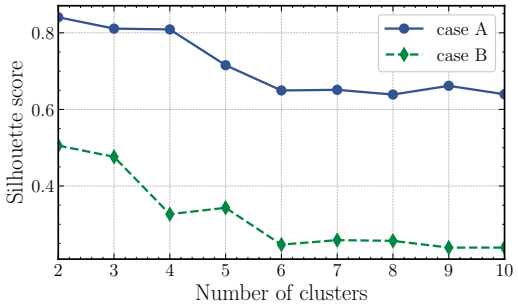

Fig. 3: Silhouette scores for cases A and B.

Cases A and B provide similar results for 3 clusters. Indeed, the 3 clusters correspond to a fresh gases zone, a burnt gases zone and an intense flame zone, respectively. This can be related to the fact that in both cases the majority of the variance is explained by a progress variable. By introducing more clusters,

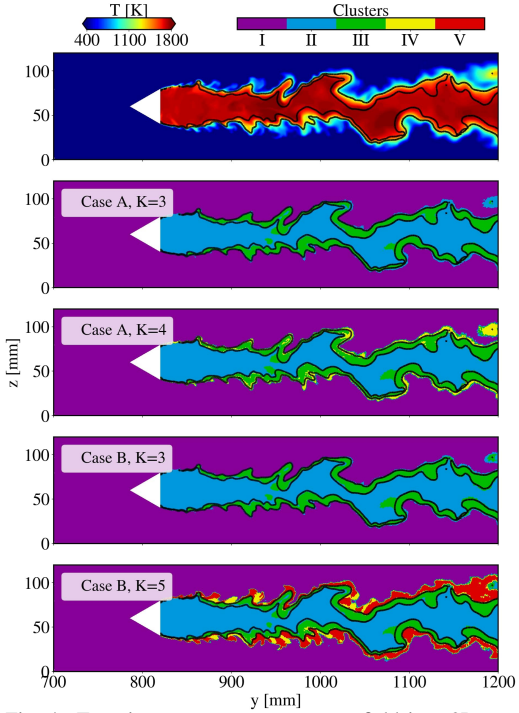

Fig. 4: Top: instantaneous temperature field in a 2D cut. Bottom: results of the K-means algorithm at the same instant for different cases. Black isoline: HRR = 0.7 $\mathrm{MJ/kg/m^3}$.

differences appear between case A and case B. In both cases, the new clusters are located between the intense flame zone and the fresh gases. For case A, the additional cluster corresponds to a preheat zone where low intensity heat release rate occurs. On the other hand, clusters IV and V for case B are correlated with high transverse velocity, either positive or negative.

The previous discussion highlights the importance of the physical interpretation of the clusters, showing the additional features that can be retrieved with a higher number of clusters even with a lower silhouette score. As case A with 4 clusters presents more physical features and provides a high silhouette score close to the maximum, it is retained for the balance analysis discussed hereafter.

4.2. Physical analysis

The temporal evolution of the 4 case A-clusters' location during blowoff is displayed in Fig. 5. Labeling the clusters is important for the physical analysis. Feature correlation tools exist in the literature [11] but often labels are assigned following expert user knowledge [30]. In this work, the labeling is performed following the study of the mean values of temperature and species mass fractions in the clusters, reported in Table 3. Cluster 0, corresponding to fresh gases, is characterized by a low temperature, high reactant mass fractions and low product mass fractions. Conversely, cluster 2 contains burnt gases and, thus, has

the highest temperature and product mass fractions. Intermediate zones are either preheat (cluster 1) and flame (cluster 3), with intermediate values of temperature and major species. Note that the temperature is higher in the flame than in the preheat zone, and that CO mass fraction peaks in the flame zone. The labeling of the clusters is summarized in Table 4.

Table 3: Clusters' centroids in the physical space

Variables	FG	PF	BG	IF
T [K]	423	1223	1615	1484
Y_{CO}	4.6e-7	4.6e-5	1.3e-5	1.5e-4
Y_{CO2}	0.010	0.073	0.108	0.094
Y_{O2}	0.214	0.139	0.097	0.111
Y_{H2O}	0.005	0.038	0.55	0.050
Y_{C3H8}	0.029	0.009	0.0	0.007

Table 4: Physical Interpretation of the clusters

Cluster #	Interpretation	Abbrev.
0	Fresh gases	FG
1	Preheat/low intensity flame	PF
2	Burnt gases	BG
3	Intense flame	IF

As discussed in the previous section, the initial stable flame (t=2.1 ms) features three main clusters: the fresh gases (cluster 0 - FG), the burnt gases (cluster 2 - BG) and the intense flame zone (cluster 3 - IF), plus a preheat zone at the border of the intense flame zone (cluster 1 - PF). At t=4.7 ms, the equivalence ratio decrease has reached the flame stabilization zone downstream of the bluff body, and starts to perturb the flame (cluster 3 - IF), which shrinks and is replaced by heated, low reacting gases (cluster 1 - PF). This perturbation, i.e., switch from IF to PF, then propagates downstream with the propagation of the equivalence ratio decrease until t=11.9 ms. At this point, the zone of burnt gases (cluster 2 - BG) divides into two disconnected parts. The part of burnt gases upstream, which persists within the recirculation zone immediately after the bluff body, is surrounded by PF and gradually diminishes, while the detached downstream part of burnt gases swiftly evacuates due to the flow.

From this analysis, a first proposition can be made to define a criterion of extinction. Indeed, in this configuration the flame is anchored in the recirculation zone downstream the bluff body. In other words if the flame disappears in this zone, global quenching occurs. This corresponds to no IF in the recirculation zone, which can be taken as an extinction criterion and in the present case occurs at τ_{LBO} = 13.2 ms. The use of clusters therefore allows to easily and clearly identify global extinction which, as will be seen below, is not possible with the single time evolution of global quantities [2].

This is illustrated in Fig. 6 showing the time evolution of key quantities of interest. After 6 ms, the thermal power and mean temperature both decrease linearly with time and completely ignore the extinction event at τ_{LBO}=13.2 ms. This is due to the fact

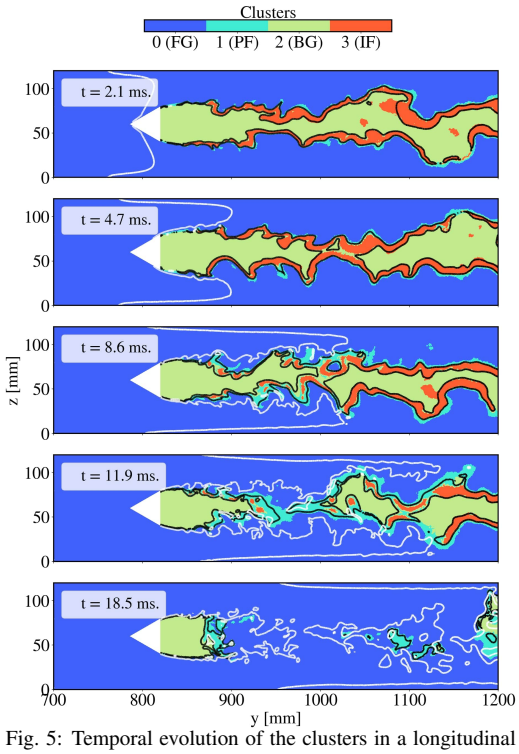

Fig. 5: Temporal evolution of the clusters in a longitudinal cut in case A with 4 clusters. Black isoline: HRR = 0.7 $\mathrm{MJ/kg/m^3}$. White isoline: $\Phi = 0.51$.

that global extinction always starts in a small volume and is masked by the volumes of the burnt gases and of the flame, which decrease progressively. It is also interesting to look at the maximum CO mass fraction which, as seen above, is a good marker of IF. The CO mass fraction also decreases with an average constant slope, but contrary to the two previous quantities it decreases from the beginning and, at t=24ms, it abruptly goes close to zero. This different behavior is due to the fact that, because CO mostly exists in IF, there is no masking effect by the rest of the chamber volume. The sudden final decrease is linked to the sweeping of the last remaining pocket out of the chamber.

Cluster analysis may be used to go deeper in the understanding of the occurrence of quenching by establishing energy and mass balances of clusters as proposed in Section 2.2. The analysis logically focuses on the first 12 ms, i.e., before extinction occurs.

Figure 7 displays the analysis of the rate of change of total energy in PF for each contribution term described in Section 2.2. The net convective flux remains at a constant level over time. This means that the flow dynamics in the shear layer where PF is located is not perturbed by the variation in equivalence ratio. On the contrary, the balance between conductive heat flux and chemistry is perturbed after 4 ms as it starts decreasing. This means that the convective characteristic time of the flow stays almost con-

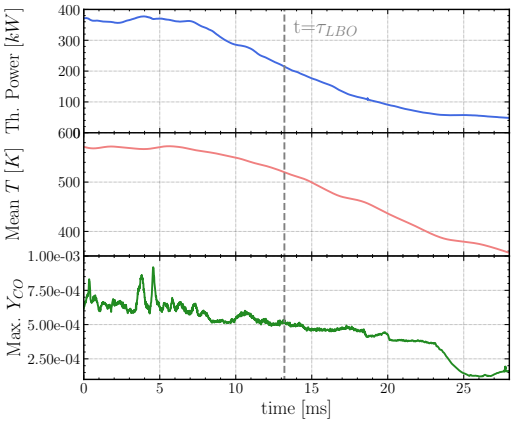

Fig. 6: Temporal evolution of the thermal power, mean temperature and maximum CO mass fraction during extinction.

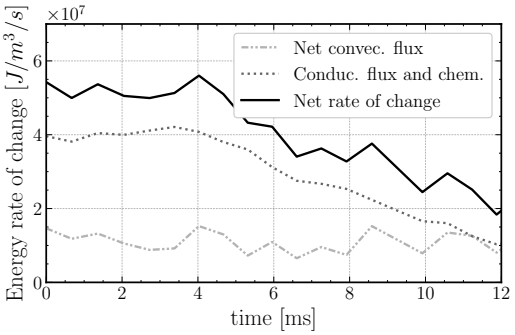

Fig. 7: Temporal evolution of the total energy rate of change by contribution terms for cluster 1 (PF).

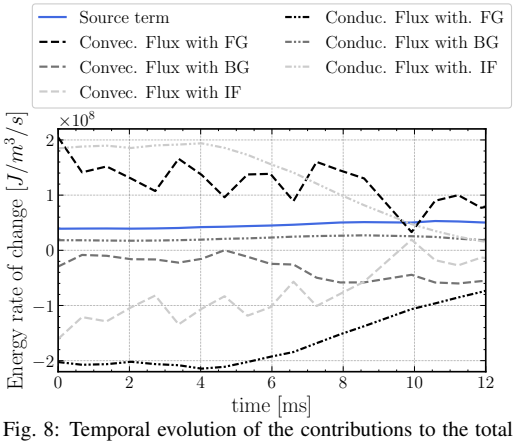

Fig. 8: Temporal evolution of the contributions to the total energy rate of change for cluster 1 (PF).

stant whereas the characteristic time for chemistry increases. This conclusion is similar to the classical local analysis in terms of Damkhöler number but expressed in a global framework.

The rate of change of the total energy can be further studied by highlighting the contribution of each cluster, as shown in Fig. 8. This graph clearly shows that the decrease in the chemistry - conduction balance in the energy rate of change of Fig. 7 is mainly due to the sharp reduction of the conductive energy provided by IF. Even though the net convective flux remains quasi-constant, the contribution to this flux from each cluster changes over time. At first, when the flame is stabilized, PF exchanges mainly with FG and IF. But during extinction, as IF tends to be replaced by PF in the recirculation zone, its contribution to the convective flux reduces, progressively replaced by an increasing convective flux from BG, which is more and more in contact with PF in the recirculation zone.

Finally, a deeper analysis of the changing conduction - chemistry balance can be made by considering the time evolution of the CO mass rate of change for the clusters PF and IF (Fig. 9). Note that the contributions are normalized by the cluster volume, which explains why the value of the same flux may change from one graph to another. PF is the first cluster impacted by the decrease of equivalence ratio at t=4 ms, when both the CO flux from IF and the source term start decreasing in absolute value. This decrease continues until 10 ms when the source term changes sign and becomes positive in PF. This may be associated to a change of mechanism. In a stable flame, PF acts mainly as a preheat zone between FG and IF, where CO produced in IF is consumed. During extinction, after a certain time (see Fig. 5, t=8.6 ms), an increasing part of PF lies between FG and BG with lower CO mass fraction and CO may be produced. The cluster IF reacts to the change of equivalence ratio later than PF, after 6 ms. The source term has a sharper decrease than the diffusive fluxes, which explains why IF tends to disappear.

The above cluster analysis agrees with previous results in the literature [2]: when decreasing the equivalence ratio in the inlet stream, the exchange through convection is maintained whereas the balance between the chemistry (studied through the rate of change of total energy and CO mass fraction coming from the source term) and diffusive terms is perturbed. This affects mainly the two clusters located in the shear layer, cluster 1 (PF) and cluster 3 (IF): PF sees a reduction in the net rate of change of the total energy mainly driven by the reduction of the conductive flux coming from IF.

5. Conclusions

A balance analysis that relies on unsupervised classification is applied to study the lean blow-out of a bluff body configuration, the VOLVO combustor. The unsupervised classification, coupling PCA and K-means algorithms, is first discussed with a particular emphasis on the physical meaning that could be retrieved from the classification. If fresh gases and burnt gases are easily recognized, the classification also identifies reactive zones as key features in the flow. This allows to identify a blowoff criterion, based

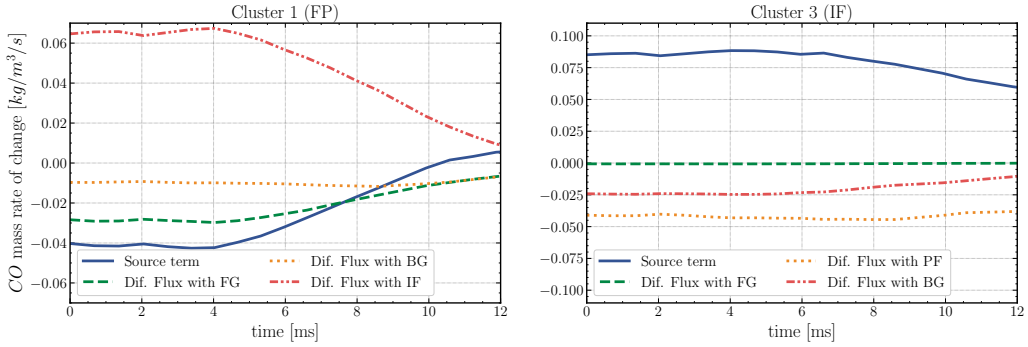

Fig. 9: Temporal evolution of the contributions to the CO mass rate of change for clusters 1 (PF) and 3 (IF).

on the total disappearance of the flame cluster in the recirculation zone downstream the bluff body.

The balance analysis performed on the clusters shows that the decrease of equivalence ratio in an extinction sequence impacts the balance between chemistry and diffusive fluxes in the preheat and flame zones located in the recirculating flow downstream the bluff body whereas the convection contribution remains constant.

Compared to the classical reactor network analysis with non-time-dependent zones, which requires user-dependent, i.e., biased choices, the present work offers a non-biased method to define coherent zones in the flow through the use of unsupervised classification. In addition, the present methodology particularly emphasizes how a change in the system affects the unsteady balance between the zones, which is key for understanding extinction.

This paper demonstrates the capability of the coupling of unsupervised classification and balance analysis to study unsteady phenomena, like lean blow out. This methodology offers a new framework to study and understand the underlying mechanisms of complex unsteady flows and, therefore, opens the perspective to use this method in other contexts such as LBO in swirled turbulent flames, forced ignition, etc.

Declaration of competing interest

The authors declare that they have no known competing financial interests or personal relationships that could have appeared to influence the work reported in this paper.

Acknowledgments

This work was performed using HPC resources from GENCI-TGCC (Grant 2023-A0132B10157). We also acknowledge the EuroHPC Joint Undertaking for awarding this project access to the EuroHPC supercomputer LUMI, hosted by CSC (Finland) and the LUMI consortium through a EuroHPC Regular Access call.

References

[1] V. McDonell, Chapter 5 - lean combustion in gas turbines, in: D. Dunn-Rankin (Ed.), Lean Combustion, Academic Press, Burlington, 2008.

[2] S. J. Shanbhogue, S. Husain, T. Lieuwen, Lean blowoff of bluff body stabilized flames: Scaling and dynamics, Prog. Energy Combust. Sci. 35 (1) (2009) 98–120.

[3] L. Esclapez, P. C. Ma, E. Mayhew, R. Xu, S. Stouffer, T. Lee, H. Wang, M. Ihme, Fuel effects on lean blow-out in a realistic gas turbine combustor, Combust. Flame 181 (2017) 82–99.

[4] D. R. Ballal, A. H. Lefebvre, Weak extinction limits of turbulent flowing mixtures, J. Eng. Pow. 101 (1979) 343–348.

[5] J. P. Longwell, E. E. Frost, M. A. Weiss, Flame stability in bluff body recirculation zones, Ind. Eng. Chem. 45 (8) (1953) 1629–1633.

[6] E. E. Zukoski, F. E. Marble, Combustion researches and reviews, AGARD, Butterworths, 1955.

[7] Z. Wang, B. Hu, A. Fang, Q. Zhao, X. Chen, Analyzing lean blow-off limits of gas turbine combustors based on local and global damköhler number of reaction zone, Aerosp. Sci. Technol. 111 (2021) 106532.

[8] G. Sturgess, D. Shouse, A hybrid model for calculating lean blowouts in practical combustors, 1996.

[9] S. Bragg, Application of reaction rate theory to combustion chamber analysis, Tech. rep., Aeronautical Research Council, London (England) (1953).

[10] S. Correa, K. Overton, A model for optimizing emissions and stability of a gas-turbine combustor, 1988.

[11] M. Rovira, K. Engvall, C. Duwig, Identifying key features in reactive flows: A tutorial on combining dimensionality reduction, unsupervised clustering, and feature correlation, Chem. Eng. J. 438 (2022) 135250.

[12] M. Savarese, A. Cuoci, W. De Paepe, A. Parente, Machine learning clustering algorithms for the automatic generation of chemical reactor networks from cfd simulations, Fuel 343 (2023) 127945.

[13] M. R. Malik, R. Khamedov, F. E. Hernández Pérez, A. Coussement, A. Parente, H. G. Im, Dimensionality reduction and unsupervised classification for high-fidelity reacting flow simulations, Proc. Combust. Inst. 39 (4) (2023) 5155–5163.

[14] H. Zhang, H. Lu, F. Xie, T. Ma, X. Qian, Combustion regime identification in turbulent non-premixed flames with principal component analysis, clustering and back-propagation neural network, Processes 10 (8) (2023) 1653.

[15] H. Dave, N. Swaminathan, A. Parente, Interpretation and characterization of mild combustion data using unsupervised clustering informed by physics-based, domain expertise, Combust. Flame 240 (2022) 111954.

[16] Z. Li, S. Tomasch, Z. X. Chen, A. Parente, I. S. Ertesvåg, N. Swaminathan, Study of mild combustion using les and advanced analysis tools, Proc. Combust.

Inst. 38 (4) (2021) 5423–5432.
[17] A. Sjunnesson, S. Olovsson, B. Sjoeblom, Validation rig-a tool for flame studies, Symp. Pap. 10th Int. Symp. Air Breath. Engines 1 (1991) 385–393.
[18] C. Sammut, G. Webb, Encyclopedia of Machine Learning and Data Mining, 2nd Edition, Springer, New York, 2017.
[19] A. Dudek, Silhouette index as clustering evaluation tool, in: Classification and Data Analysis, Springer, Cham, 2020, pp. 19–33.
[20] T. Poinsot, D. Veynante, Theoretical and Numerical Combustion, 2nd Edition, R.T. Edwards Inc., Philadelphia, 2005.
[21] P. A. Cocks, M. C. Soteriou, V. Sankaran, Impact of numerics on the predictive capabilities of reacting flow les, Combust. Flame 162 (9) (2015) 3394–3411.
[22] T. Schonfeld, M. Rudgyard, Steady and unsteady flow simulations using the hybrid flow solver AVBP, AIAA 37 (11) (1999) 1378–1385.
[23] P. D. Lax, B. Wendroff, Difference schemes for hyperbolic equations with high order of accuracy, Commun. Pure Appl. Math. 17 (1964) 381–398.
[24] F. Nicoud, F. Ducros, Subgrid-scale stress modelling based on the square of the velocity gradient tensor, Flow Turbu. Combust. 62 (3) (1999) 183–200.
[25] T. Jaravel, Prediction of pollutants in gas turbines using large eddy simulation, Ph.D. Thesis, Institut National Polytechnique de Toulouse, Toulouse (2016).
[26] F. Charlette, C. Meneveau, D. Veynante, A power-law flame wrinkling model for les of premixed turbulent combustion part i: non-dynamic formulation and initial tests, Combust. Flame 131 (1) (2002) 159–180.
[27] T. Poinsot, S. Lelef, Boundary conditions for direct simulations of compressible viscous flows, J. Comput. Phys. 101 (1) (1992) 104–129.
[28] B. Franzelli, E. Riber, M. Sanjosé, T. Poinsot, A two-step chemical scheme for kerosene–air premixed flames, Combust. Flame 157 (7) (2010) 1364–1373.
[29] B. Rochette, F. Collin-Bastiani, L. Gicquel, O. Vermorel, D. Veynante, T. Poinsot, Influence of chemical schemes, numerical method and dynamic turbulent combustion modeling on les of premixed turbulent flames, Combust. Flame 191 (2018) 417–430.
[30] R. Koopman, S. Wang, Mutual information based labelling and comparing clusters, Scientometrics 111 (2017) 1157–1167.